An assessment of attenuation correction of SPECT MPI images generated by deep learning model

Nguyen Thanh Trung[1], Dang Hoang Minh[2],
Chu Minh Duc[3], Pham Ha Hai[1], Nguyen Chi Thanh[2*]

[1] Department of Medical Equipment, 108 Military Central Hospital, Hanoi, Vietnam;
[2] Institute of Information Technology, AMST, Hanoi, Vietnam;
[3] Department of Nuclear Medicine, 108 Military Central Hospital, Hanoi, Vietnam.
*Corresponding author: thanhnc80@gmail.com.
Received 9 September 2021; Revised 12 December 2021; Accepted 15 December 2021.
DOI: https://doi.org/10.54939/1859-1043.j.mst.csce5.2021.93-101

ABSTRACT

This article evaluates the effectiveness of using a deep learning network model to generate reliable attenuation corrected the single-photon emission computed tomography (SPECT) myocardial perfusion imaging (MPI). The authors collected myocardial perfusion imaging data of 88 patients from a SPECT/CT machine, with an average age of 62.47 years. Then, two datasets are created from the original data: set A includes the deep learning-based attenuation corrected images (Generated Attenuation Correction - GenAC), and the non-attenuation corrected images; set B contains only non-attenuation corrected images. These datasets were diagnosed by two doctors (in which, one has 7 years of experience and the other has 10 years of experience in reading SPECT MPI). The doctors diagnose based on the image data without knowing which dataset it belongs to. The sensitivity, specificity, diagnostic accuracy, and lesion rate were evaluated between the two data sets. Results: The average specificity, sensitivity, and accuracy of the set with the deep learning-based attenuation corrected images were 0.87, 0.86, 0.86, while the results with the non-attenuation corrected images are 0.69, 0.83, and 0.78.

Keywords: Single photon emission computed tomography (SPECT); Attenuation Correction (AC); Non-Attenuation Correction (NC); Deep Learning (DL); Computer-aided diagnosis (CAD); Myocardial Perfusion Imaging (MPI).

I. INTRODUCTION

Coronary artery disease (CAD) is one of the diseases of concern today because the number of individuals with coronary artery disease is increasing. Arterial diseases can result in many serious complications, including heart attack, stroke, aneurysm, and even death. Furthermore, the costs of treating coronary artery disease are relatively high, particularly for people with advanced illness or a complicated medical history. As a result, early diagnosis and detection of coronary artery disease help treat patients more effectively, increase survival overall and reduce treatment costs. Myocardial perfusion imaging (MPI) with a SPECT camera is used to diagnose coronary artery disease. The accuracy of diagnosis depends on many factors, including the quality of the images, the doctor's expertise, and experiences. One way to improve accuracy in diagnosing coronary artery disease is to use machine learning to enhance the imaging quality.

Many studies have proved the value of SPECT myocardial perfusion imaging in detecting coronary artery disease [1-3]. However, the leading cause of lower diagnostic accuracy is attenuated noise caused by soft tissue density variations. Attenuating noise causes areas of attenuation on cardiac SPECT pictures, making it harder to discern between coronary artery disease and attenuated noise and lowering the method's specificity. As a result, there are false positives in the diagnostic. [4]

Recently, the most efficient approach to reduce attenuation noise on cardiac SPECT images is using a CT tomography scanner to create a degradation map. This method has many limitations, such as cost rising for equipment and additional radiation dose for patients. Furthermore, the number of SPECT/CT machines is limited, accounting for only around 20% of all SPECT machines globally [5, 6]. Therefore, a machine learning model for attenuation noise reduction has been suggested and demonstrated to be equivalent to the CT slicer approach. However, this approach has yet to be verified by doctors using SPECT technology in the field of myocardial perfusion imaging.

In this study, we compare the diagnostic results of two physicians with attenuation-corrected cardiac SPECT images generated by a deep learning model, CT-based attenuation corrected cardiac SPECT images, and uncorrected cardiac SPECT images.

2. METHOD

2.1. Cardiac SPECT images and attenuation correction

Cardiac SPECT images were obtained after performing myocardial perfusion imaging with SPECT machine according to the Bruce procedure under the guidelines of the American Society of Nuclear Cardiology ASNC. 60 minutes before the image scan, the patient was injected with the radionuclides Tc99m MIBI at a dose of 0.31mCi/kg for both resting and stress phases. Dipyridamole is used at a dose of 0.56 mg/kg/ 4 min after the heart rate reaches the theoretical 85% in patients with contraindications to vigorous exercise.

GE Healthcare's SPECT machines include the Optima 640, Infinia, and Ventri. According to GE guidelines, the procedure and image settings were configured by default. Doctors inspect image quality using specialized software such as QGS/QPS on Xeleris servers. Figure 1 is the cross-sectional images taken during a myocardial perfusion scan session.

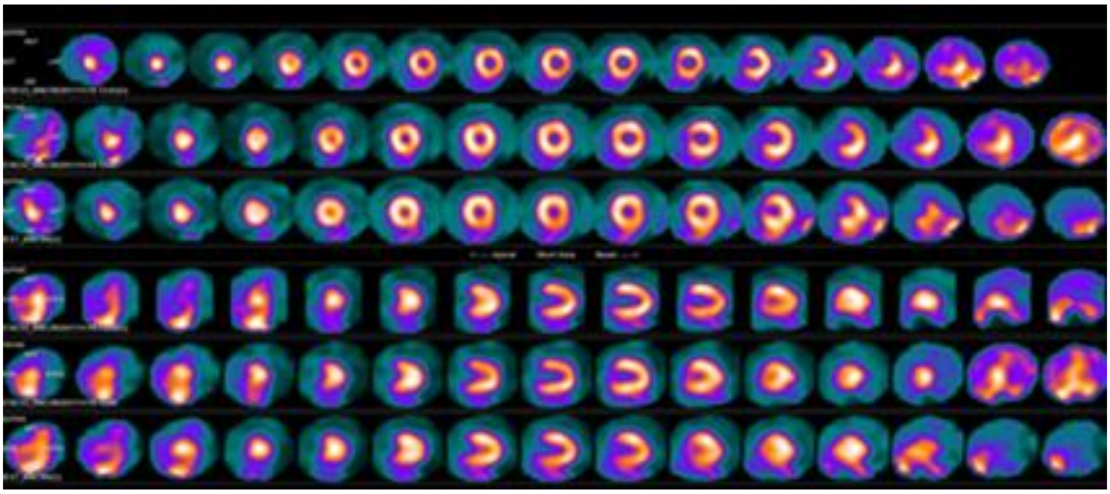

***Figure 1**. The cross-sectional images taken during a myocardial perfusion scan session.*

Images quality is critical in myocardial perfusion imaging using SPECT equipment. The attenuating caused by the density variation of the tissues is responsible for the non-coronary radial defects on cardiac SPECT imaging, resulting in reduced image quality and accuracy diagnosis [1-3].

Currently, the most effective method to correct attenuation noise is to combine the CT system with the conventional SPECT machine to create a SPECT/CT machine. This method works on the principle of using X-rays to scan the patient's body and create a map of tissue degeneration. Then, using complicated reconstruction methods, the attenuation map is integrated with the SPECT imaging without NC degradation correction to create images with AC degradation correction (figure 2). This method has been demonstrated to be better than prone methods combined with an ECG [5-7].

However, combining CT with SPECT to create a SPECT/CT system increase the cost of the machine. Also, radiation safety or radiation dose for patients is more challenging with a SPECT/CT system. Furthermore, conventional SPECT machine systems, which do not include the CT attenuation correction capability, account for 80% of the world's SPECT machine systems. Only big Nuclear Medicine centers in Vietnam have SPECT/CT equipment.

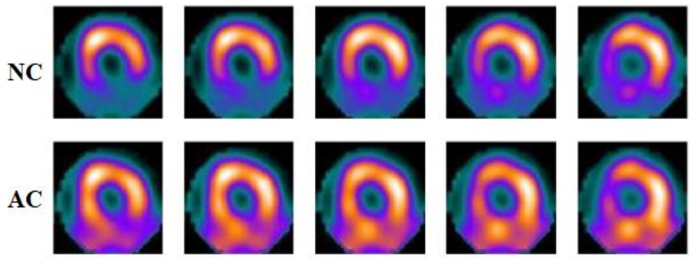

Figure 2. *The SPECT images without NC attenuation correction and AC attenuation correction.*

A recently developed deep learning model is used to correct attenuation in conventional SPECT images. The quality of the attenuation corrected image obtained by this method is comparable to that of the CT machine [19]. However, this method of attenuation correction by this model requires the evaluation of doctors in Nuclear Medicine.

2.2. Attenuated correction using a deep learning model

In previous researches [19], the authors developed a deep learning network model based on GAN and U-Net network architecture to perform attenuation correction. The model uses 3D CNN layers to capture the connection between adjacent slice images. We create a three-dimensional GAN model with U-Net network architecture as the generating network employing 3D CNN layers as the major component. All of the 3D CNN layers in the model have the same kernel size (3x3x3), stride 2, and use the ReLU activation function. The model's network architecture is depicted in figure 3.

Generator Network: 28 sequential slice images with each image size (90x90x3) are combined to generate a data sample with size (28x90x90x3) used as input to the generator network. If there aren't enough slices to create a sample, zero-value slices are added to make sure they're all the same size.

Network Compare: Discriminator is designed to discriminate between the attenuation corrected images created from the generating network, and the attenuation corrected images by CT of NC images. Therefore, each NC image is merged with the corresponding AC image to form a new slice image with the size of (90x90x6). We build a comparator - discriminator with 6 3D-CNN layers with the kernel size of (2x2x2), stride 2 (except the last 2 layers with stride 1). Each 3D CNN layer is followed by a Batch Normalization Layer and a Leaky ReLU activation function.

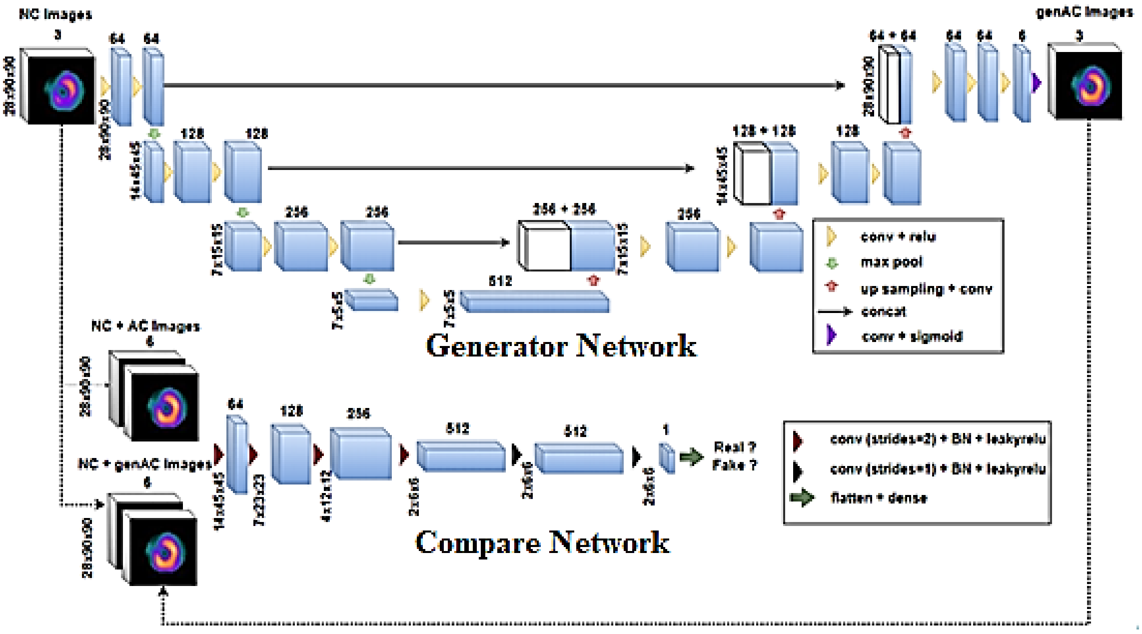

Figure 3. *The model's network architecture.*

The authors used the trained model from the study [19] to create attenuation corrected images (GenAC). The attenuation corrected images will be evaluated by the doctor's diagnostic process. The evaluation's results estimate the ability of GenAC images to improve diagnostic accuracy over NC images.

2.3. Evaluation methods

First, the authors create attenuation corrected image data for 3 axes: short axis, vertical axis, and horizontal axis. To support doctors in the diagnostic process on these attenuation corrected images, the authors developed special software (figure 4) familiarly showing the images with doctors. The software shows the doctor cross-sectional images of three axes: the short axis, the vertical axis, and the horizontal axis. These axes include AC images of the stress phase, NC images of the rest, and tress phase. The doctors label the cases as lesions or no lesions. If a patient is diagnosed with a lesion, the doctors determine the location of lesions: the left anterior descending (LAD), the circumflex artery (LCX), or the right coronary artery (RCA).

We created two data sets of the same patients with the structure of each set as in table 1: Set A contains both GenAC and NC images, while set B contains only NC images. We created two data sets of the same patients with the structure of each set as in table 1. Each data sample includes slice images from a specific patient. During the evaluation phase, the doctors diagnose the patients based on the images from the two data sets in table 1.

Table 1. *Two data sets in the experiment.*

Image sets	Image type
Set A	NC + GenAC
Set B	NC

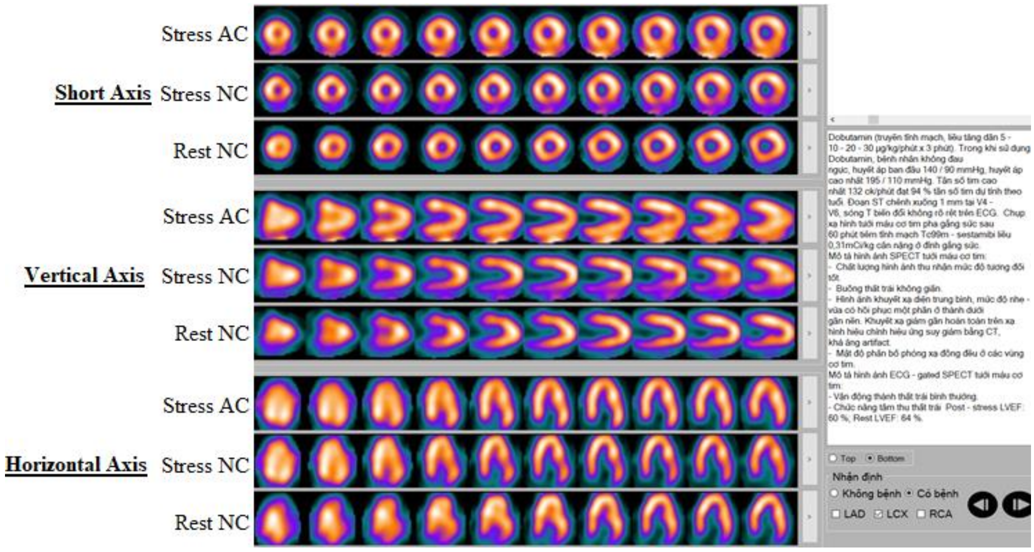

Figure 4. *Software to support reading results in experiments.*

3. EXPERIMENT AND RESULTS

3.1. Experiment data

The data of 88 patients from 2017 to 2019 were collected at the 108 Military Central Hospital's Department of Nuclear Medicine. These patients must satisfy two criteria: they must be from the test data set in the authors' prior studies [18, 19] and have rest and stress imaging data. Tables 2 and 3 provide more information on the dataset. These 88 patient data were used to help doctors diagnose and treat coronary artery disease.

The personal data of each patient, such as name, address, date of photography, and the information part, have been removed to ensure objectivity in the assessment of the image files and to avoid the phenomena of the doctor remembering the patient. The previous diagnosis results were also removed. The data include SPECT cardiac images and patient information in the process of pre-perfusion imaging with a SPECT machine.

Table 2. *Statistics of patient information.*

	Quantity	**Ratio (%)**
The average age	62.47	
Male	66	75
Female	22	25
Hypertension	49	55.68
Heart failure	6	6.8
Left chest pain	79	89.77
Diabetes	13	14.7
Myocardial infarction	1	1.1
Use stent	7	7.9
Total number of patients	**88**	

Table 1. *Statistics of coronary artery disease types in the data set.*

	Quantity
Negative	59
Positive	29
LAD	23
LCX	9
RCA	13
Total number of patients	**88**

Each patient's NC images are input into the deep learning model in the study [19] to create GenAC images. Figure 3 shows the model's architecture, which includes 3D CNN layers to assist in detecting the relation between adjacent slice images. A generator with a U-Net design creates corrected slice images from an uncorrected input image. Data for sets A (NC images and images corrected by the deep learning model) and B (NC images) are created from the 88 patients.

3.2. Experiment settings

The authors cooperated with two doctors from the 108 Military Central Hospital's Department of Nuclear Medicine. The first doctor (Doctor 1) has ten years of experience, while the second (Doctor 2) has seven years of experience diagnosing SPECT-based myocardial perfusion imaging.

Two doctors will label the data from sets A and B whether the imaging data belongs to the positive or negative group.

3.3. Result

Table 4 displays the analysis results. When comparing the diagnostic results on the set of experiments, it showed that the diagnostic accuracy of the two doctors with Set A increased significantly, up to 8%, in identifying cardiac disease. It means GenAC images could help doctors diagnose more accurately than NC images only.

Figures 5 and 6 compare the two doctors' diagnosis results in two data sets. In terms of sensitivity and specificity on each patient, these figures also show that Set A of NC images and GenAC images gives better results than using NC images only.

When compared to Set B, the sensitivity and specificity of Set A are improved. This demonstrates that diagnosing using additional GenAC images generated by the attenuation corrected image prediction model is more effective than NC images only. The specificity when using GenAC images of Doctor 1 and Doctor 2 increased by 11% and 25%, respectively. The difference in specificity improvement between the 2 doctors could be explained by the fact that Doctor 1 had more years of experience than Doctor 2. Sensitivity rose by 3% for both doctors due to the efficient information from GenAC images.

Table 2. *Diagnostic results of two doctors.*

	Set A - Gen AC			**Set B - NC**		
	Accuracy	Specificity	Sensitivity	Accuracy	Specificity	Sensitivity
Doctor 1	0.85	0.83	0.86	0.79	0.72	0.83
Doctor 2	0.875	0.91	0.86	0.77	0.66	0.83
Average	0.8625	0.87	0.86	0.78	0.69	0.83

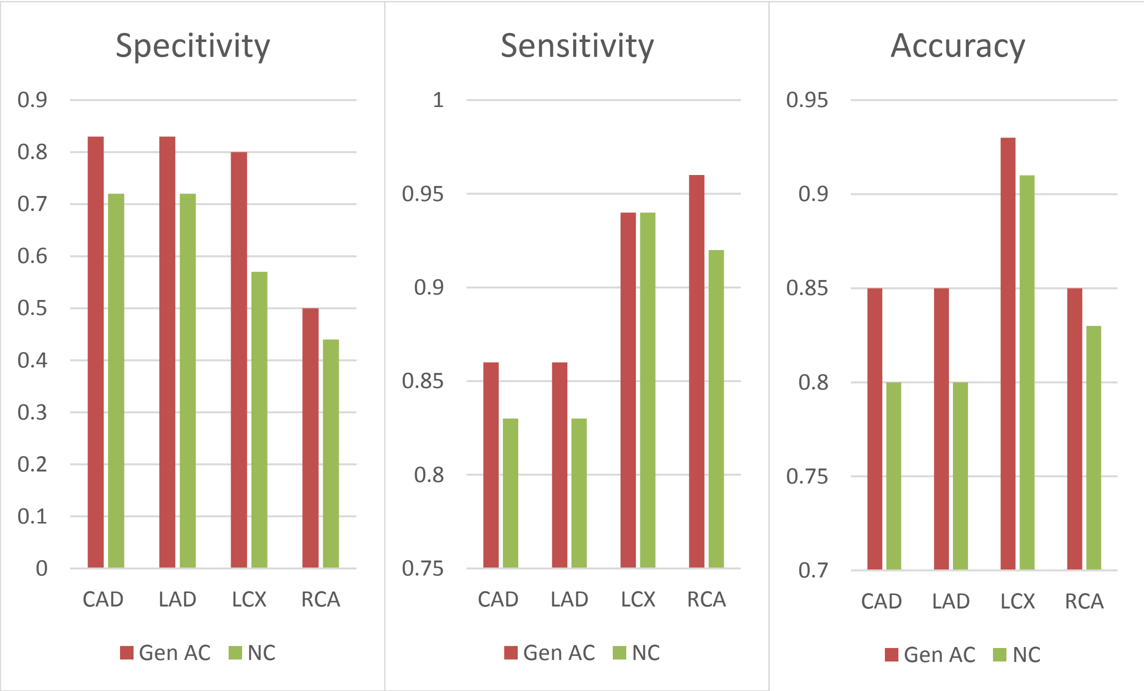

Figures 1. *Comparison of the results of Doctor 1.*

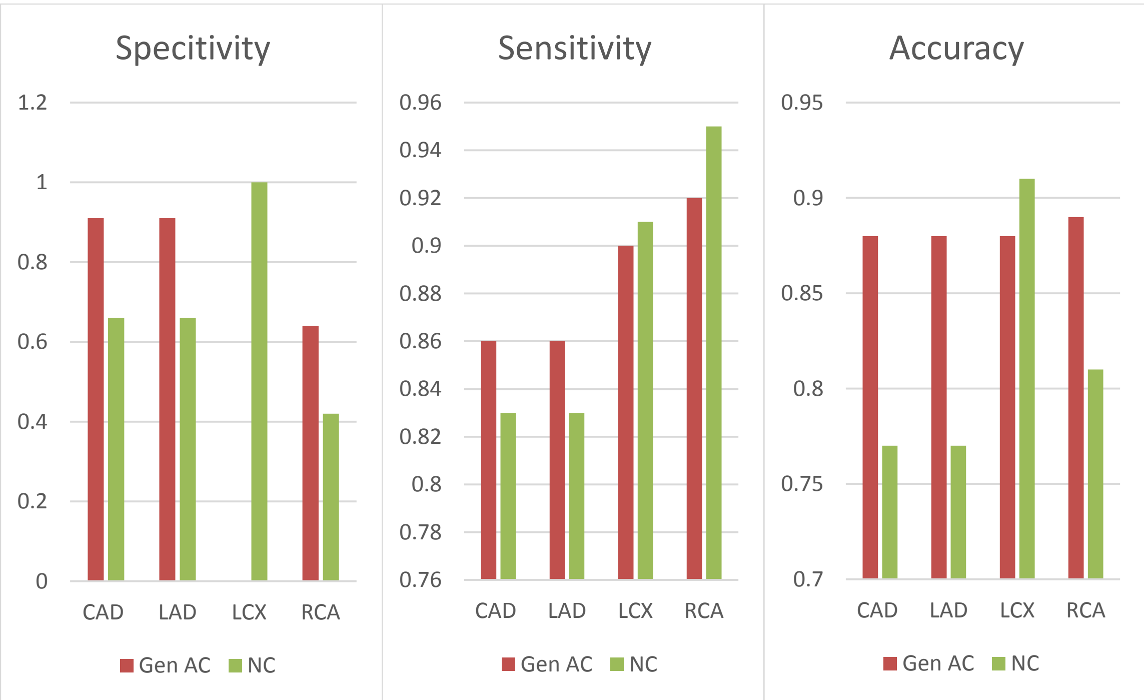

Figures 2. *Comparison of the results of Doctor 2.*

The detection rate of patients without lesions increased significantly for Doctor 1 by 5.09% and up to 13.11% for Doctor 2 when using more GenAC images than only NC images. So GenAC images support cardiac SPECT imaging for less experienced doctors, significantly increasing the detection rate of patients without lesions.

4. CONCLUSION

This research evaluates a method for generating images with GenAC attenuation correction for SPECT machines that do not have a CT attenuation correction feature using the 3D UNet GAN deep learning model. With an increased accuracy of 8%, sensitivity of 3%, and specificity of 18%, this method assists doctors in improving the diagnosis of coronary artery disease.

As a result, early detection and diagnosis of coronary artery disease could be more accurate and effective, allowing doctors to detect the disease earlier and choose the best treatment to retain good health while saving the patient's money. This approach helps medical facilities to save costs without requiring CT machines or other operating expenditures; patients also don't get high radiation doses and complicated problems while undergoing SPECT/CT procedures.

REFERENCES

[1]. Goff D. C., Jr., et al, *"2013 ACC/AHA guideline on the assessment of cardiovascular risk: a report of the American College of Cardiology"*, American Heart Association Task Force on Practice Guidelines, Circulation, 129, 25 Suppl 2, Jun. 2014, 49-73, doi: 10.1161/01.cir.0000437741.48606.98.

[2]. Einstein AJ, *"Effects of radiation exposure from cardiac imaging: how good are the data?"*, J Am Coll Cardiol 59, 2012, pp. 553–565, doi: 10.1016/j.jacc.2011.08.079

[3]. Peter L. Tilkemeier, MD, *"Standardized reporting of radionuclide myocardial perfusion and function"*, Journal of Nuclear Cardiology (2009), doi: https://doi.org/10.1007/s12350-009-9095-8.

[4]. Bateman TM, Dilsizian V, Beanlands RS, DePuey EG, Heller GV, Wolinsky DA, *"American society of nuclear cardiology position statement"*, Journal of Nuclear Cardiology, 2016, doi:10.1007/s12350-016-0626-9.

[5]. Technavio (2017), *"Global SPECT Market 2017-2021"*, https://www.technavio.com/report/globalmedicalimagingglobalspectmarket2017-2021

[6]. Jha AK, Zhu Y, Clarkson E, Kupinski MA, Frey EC (2018), *"Fisher information analysis of list-mode SPECT emission data for joint estimation of activity and attenuation distribution"*, arXiv preprint. arXiv:180701767.

[7]. Hesse B, et al, "*EANM/ESC procedural guidelines for myocardial perfusion imaging in nuclear cardiology"*, European journal of nuclear medicine and molecular imaging, 32(7), 2005, pp. 855-897, doi: 10.1007/s00259-005-1779-y.

[8]. Holly T. A., et al, *"Single photon-emission computed tomography"*, J Nucl Cardiol, 17(5), 2010, pp. 941-973, doi: 10.1007/s12350-010-9246-y.

[9]. Chien-Shun Lo, Chuin-Mu Wang, *"Support vector machine for breast MR image classification"*, Computers & Mathematics with Applications, Volume 64, Issue 5, 2012, pp. 1153-1162, doi: 10.1016/j.camwa.2012.03.033.

[10]. Z. Camlica, H. R. Tizhoosh and F. Khalvati, *"Medical Image Classification via SVM Using LBP Features from Saliency-Based Folded Data,"* 2015 IEEE 14th International Conference on Machine Learning and Applications (ICMLA), Miami, FL, 2015, pp. 128-132, doi: 10.1109/ICMLA.2015.131.

[11]. Jiang, Yun & Li, Zhanhuai & Zhang, Longbo & Sun, Peng, *"An Improved SVM Classifier for Medical Image Classification"*, 2007, pp. 764-773, doi: 10.1007/978-3-540-73451-2_80.

[12]. Hongkai Wang, Zongwei Zhou, *"Comparison of machine learning methods for classifying mediastinal lymph node metastasis of non-small cell lung cancer from 18F-FDG PET/CT*

images", EJNMMI Research, 2017, doi: 10.1186/s13550-017-0260-9.

[13]. Ryo Nakazato, Balaji K. Tamarappoo, Xingping Kang, Arik Wolak, Faith Kite1, Sean W. Hayes, Louise E.J. Thomson, John D. Friedman, Daniel S. Berman and Piotr J. Slomka, *"Quantitative Upright–Supine High-Speed SPECT Myocardial Perfusion Imaging for Detection of Coronary Artery Disease: Correlation with Invasive Coronary Angiography"*, Journal of Nuclear Medicine, vol. 51(11), 2010, pp. 1724-1731, doi: 10.2967/jnumed.110.078782.

[14]. Yann LeCun, Yoshua Bengio & Geoffrey Hinton, *"Deep learning"*, Nature, vol. 521(7553) 2015, pp. 436-444, doi: 10.1038/nature14539.

[15]. Varun Gulshan, PhD; Lily Peng, MD, PhD; Marc Coram, PhD; et al, *"Development and Validation of a Deep Learning Algorithm for Detection of Diabetic Retinopathy in Retinal Fundus Photographs"*, JAMA, vol. 316(22), Dec. 2016, pp. 2402-2410, doi: 10.1001/jama.2016.17216.

[16]. Betancur, Commandeur, Motlagh, *"Deep Learning for Prediction of Obstructive Disease from Fast Myocardial Perfusion SPECT"*, JACC: Cardiovascular Imaging, vol. 11(11), 2018, pp. 1654-1663, doi: 10.1016/j.jcmg.2018.01.020.

[17]. Karen Simonyan, Andrew Zisserman, *"Very Deep Convolutional Networks for Large-Scale Image Recognition"*, ICLR (2015).

[18]. Nguyễn Thành Trung, Nguyễn Chí Thành, Đặng Hoàng Minh, Nguyễn Thái Hà, Nguyễn Đức Thuận, *"3D Convolutional Auto-Encoder for Attenuation Correction of Cardiac SPECT Images",* Proceedings of the 2020 IEEE Eighth International Conference on Communications and Electronics (ICCE2020), 2021,

[19]. Nguyễn Thành Trung, Nguyễn Chí Thành, Đặng Hoàng Minh, Nguyễn Thái Hà, Nguyễn Đức Thuận (2020). *"3D Unet Generative Adversarial Network for Attenuation Correction of Spect Images".* Proceedings of the 2020 4th International Conference on Recent Advances in Signal Processing, Telecommunications & Computing (SigTelCom2020), Vietnam, Aug 2020, doi: 10.1109/SigTelCom49868.2020.9199018

TÓM TẮT

ĐÁNH GIÁ HIỆU QUẢ MÔ HÌNH HIỆU CHỈNH NHIỄU SUY GIẢM TRONG CHỤP XẠ HÌNH TƯỚI MÁU CƠ TIM BẰNG MÁY SPECT

Bài báo thực hiện thử nghiệm đánh giá hiệu quả việc sử dụng mô hình mạng học sâu để lọc nhiễu suy giảm cho các ảnh lát cắt trong xạ hình tưới máu cơ tim bằng máy SPECT theo độ nhạy, độ đặc hiệu và độ chính xác. Nhóm tác giả thu thập dữ liệu ảnh từ 88 bệnh nhân được chỉ định chụp xạ hình tưới máu cơ tim (MPI) bằng máy SPECT/CT với độ tuổi trung bình là 62.47 tuổi. Sau đó, hai tập dữ liệu được tạo ra từ dữ liệu gốc ban đầu: tập A bao gồm những ảnh được hiệu chỉnh bằng mô hình học sâu (Generated Attenuation Correction – GenAC) và các ảnh chưa được hiệu chỉnh nhiễu suy giảm NC; tập B chỉ gồm những ảnh NC. Các bộ dữ liệu này được chẩn đoán bởi hai bác sĩ có ít nhất 7 năm kinh nghiệm trong đọc ảnh xạ hình tưới máu cơ tim bằng máy SPECT. Hai bác sĩ sẽ chẩn đoán dựa trên dữ liệu ảnh mà không biết ảnh đó được gán nhãn gì cũng như ảnh đó thuộc bộ dữ liệu nào. Đánh giá trực quan về độ nhạy, độ đặc hiệu, độ chính xác chẩn đoán và tỷ lệ không tổn thương giữa hai tập dữ liệu có và không có ảnh hiệu chỉnh được so sánh. Kết quả: Độ đặc hiệu, độ nhạy và độ chính xác chẩn đoán trung bình của tập có ảnh hiệu chỉnh bởi mô hình học sâu (GenAC) là 0.87, 0.86, 0.86; tập gồm các ảnh chưa được hiệu chỉnh NC là 0.69, 0.83, 0.78.

Từ khóa: Chụp cắt lớp bằng bức xạ đơn photon (SPECT); Hiệu chỉnh nhiễu suy giảm (AC); Chưa hiệu chỉnh nhiễu suy giảm (NC); Học sâu (DL); Bệnh động mạch vành (CAD); Xạ hình tưới máu cơ tim (MPI).